

The Abundance and Behavior of Viruses  
in Ancient Seawater and Modern Iron-rich Environments

Senior Thesis by

Hanna K. Liu

In Partial Fulfillment of the Requirements for the

degree of

Bachelor of Science

CALIFORNIA INSTITUTE OF TECHNOLOGY

Pasadena, California

2011

© 2011

Hanna K. Liu

All Rights Reserved

## ACKNOWLEDGEMENTS

This work was supported in part by the Caltech SURF program and sponsors Carl and Shirley Larson. The study was conceived by Woodward. W. Fischer and Victoria .J. Orphan, and research was carried out in the Orphan Laboratory at the California Institute of Technology under the mentorship of W.W.F. and V.J.O. Thanks to Matthew B. Sullivan of the University of Arizona for kindly providing Syn33a phage and Seth John for his Aquil and expertise in virus flocculation.

## ABSTRACT

The proclivity of silica for ferric hydroxide sorption sites allows for an Archean iron cycle involving iron-silica co-precipitation and deposition of banded iron formations (BIF). Considering the tendency of viruses to also sorb iron, here we investigate the possibility that viruses were involved in the iron cycle and potentially deposited in BIFs. A known concentration of Syn33a cyanophages was introduced into each media and the viral particles remaining in solution after a short centrifugation were enumerated using epifluorescence microscopy. The number of particles sequestered on the siliceous ferric oxide precipitate was estimated by difference. Similar to previous experiments, we observed a strong affinity of viral particles for iron oxides in the absence of silica. However, we also observe competitive inhibition of viral adsorption by silica, though only when silica is raised to concentrations of 670  $\mu\text{M}$ . Ultimately, our data reveal that interactions between iron, silica, and viruses would have affected virus dynamics and corresponding biogeochemistry in the Archean ocean. Similar dynamics are predicted to occur in iron-rich environments today.

## TABLE OF CONTENTS

Acknowledgements	i
Abstract	ii
Table of Contents	iii
List of Figures	iv
Chapter 1: Introduction	1
Chapter 2: Methods	6
Chapter 3: Results	13
Chapter 4: Discussion	17
Chapter 5: Conclusions	19
Bibliography	20
Appendix A: Additional Figures	24

## LIST OF FIGURES

<i>Number</i>	<i>Page</i>
<b>Figure 1</b> Flowchart of developed simulation protocol. Following addition of virus, silica, and iron to Aquil, each trial is shaken gently for iron to precipitate, then centrifuged and sampled for enumeration by epifluorescence microscopy.	7
<b>Figure 2</b> Viruses remaining in solution over 2 hours using 40 mL of synthetic seawater in a 50 mL polypropylene tube. Virus concentration reliably decreased over time from $8.8 \times 10^7$ to $6.4 \times 10^7$ viruses $\text{ml}^{-1}$ , with the exception of the 1 hour time point, which dipped unexpectedly to $6.2 \times 10^7$ . This was attributed to observational error.	10
<b>Figure 3</b> Colormap of averaged percent differences. For each trial, percent differences from starting concentrations were calculated and averaged across the triplicate. Standard deviations are listed in Figure A2.	14
<b>Figure 4</b> Comparison of epifluorescence images with and without iron addition.	15
<b>Figure 5</b> Trends in Fe 200 and 2000 $\mu\text{M}$ . Comparison of averaged percent differences between two highest concentrations of iron with increasing silica. Silica concentrations are not to scale.	16
<b>Figure A1</b> Percent differences from starting concentrations for individual experiment replicates. Since we are estimating the amount of virus flocculated by difference, counts represented here have negative percent differences.	25
<b>Figure A2</b> Standard deviations of percent differences across triplicate. The maximum deviation observed was 15.6, for the condition 80 $\mu\text{M}$ Si – 200 $\mu\text{M}$ Fe. Deviations for 2000 $\mu\text{M}$ Fe and the 670 $\mu\text{M}$ Si - 0 $\mu\text{M}$ Fe trials were particularly low. The overall standard deviation (averaged) was approximately 7.3%.	26

## 1. Introduction

Today, viruses play an important role in the microbial ecology of seawater. Present at high concentrations, they are major vectors of horizontal gene transfer and influence both community structure as well as ocean-scale biogeochemistry through the effects of lysis. Studies of viruses in modern marine environments shape our understanding of how these dynamics are generated today. A major outstanding question remains: to what degree is this understanding exportable to times past? There are good reasons to hypothesize that phage dynamics were different in ancient seawater – not solely due to evolution, but also changing environmental conditions. Chief among these are a shortage of oxygen and a dramatically different composition of seawater, in particular, far higher concentrations of iron. We offer the first experimental and theoretical attempt to understand viral dynamics under conditions that represent the Late Archean ocean and similar modern environments.

Despite their small size, viruses are extraordinarily abundant. At concentrations of approximately  $10^8$  viruses  $\text{ml}^{-1}$  in seawater, there are an estimated  $10^{31}$  infections every second in the ocean and 1-10 virus-like particles per prokaryote (Weinbauer, 2004; Suttle, 2007). Viruses are also polyvalent: viral-like particles from seawater and hot springs have been found that can transfer between all three domains of life (Chiura, 1997; Chiura, 2002) and several marine phage sequences have been found to span multiple ecosystems (Breitbart *et al.*, 2004; Short & Suttle, 2005).

The abundance and versatility of viruses allow them to play an important role in the promotion of diversity, global scale processes such as nutrient and carbon cycling, and the regulation of microbial communities. Viruses exert considerable influence on community

structure through both lysogenic and lytic lifestyles. An estimated  $10^{25}$  to  $10^{28}$  bp of DNA are transferred every year by marine phages alone (Jiang & Paul, 1998; Waldor *et al.*, 2005). This highlights the potential significance of viral dynamics for microbial evolution and diversity. Viral horizontal gene transfer is known to alter ecological niches and support essential processes such as photosynthesis (Sullivan *et al.*, 2005; Coleman *et al.*, 2006; Rohwer & Thurber, 2009). In addition to transduction, viruses enhance microbial diversity by preventing dominance of the fastest growing, most abundant organisms and supporting the coexistence of organisms with similar niches (Fuhrman, 1999; Thingstad, 2000). Viruses can also control phytoplankton blooms and influence changes in community structure after bloom collapse (Peduzzi & Weinbauer, 1993; van Hannen *et al.*, 1999; Suttle, 2007). Their role in regulating the bloom-and-bust cycles of coccolithophores potentially affects global temperatures and ocean circulation, including El Niño (Wilhelm & Suttle, 1999). Furthermore, viral lysis is thought to be an important driver of dimethyl sulfoxide release through phytoplankton mortality (Hill *et al.*, 1998; Fuhrman, 1999).

As important as grazing for a source of microbial mortality, viral lysis in surface water removes 20-40% of prokaryotes per day (Suttle, 2007). It has been demonstrated that phage alone, without any other predators, can control bacterial populations (Wilcox & Fuhrman, 1994). Because the predatorial pressure from viruses naturally gives rise to a dynamic system of host and virus strategies, viruses are a natural driving force for evolution (Bidle *et al.*, 2007; Frada *et al.*, 2008; Rohwer & Thurber, 2009). Viral lysis also plays an important role in biogeochemical cycles by short-circuiting the microbial loop, enhancing carbon and nutrient recycling (Gobler *et al.*, 1997; Wilhelm & Suttle, 1999;

Poorvin *et al.*, 2004; Suttle, 2005; Brussaard *et al.*, 2008). An estimated quarter of primary production in the ocean is shunted this way, and the viral shunt is thought to sequester three gigatonnes of carbon annually, increasing the efficiency of the biological pump (Suttle, 2007).

Yet it is still unclear how these viral dynamics played out in the past. Ancient viruses have proven to be elusive. Because of their size and composition, viruses have not been detected in the fossil record, although some indirect evidence from amber inclusions suggests that viruses were present up to 100 million years ago (Poinar & Poinar, 2005). It is also possible to detect biosignatures of membrane lipids that survive diagenesis (Brocks *et al.*, 1999; Brocks *et al.*, 2003), but this may be difficult to trace specifically to viruses. Phylogenetic studies, however, point to ancient viral origins (Hendrix *et al.*, 1999; Filee *et al.*, 2002; Holmes, 2003; Benson *et al.*, 2004; Rice *et al.*, 2004). It is hypothesized that viruses arose around the same time as the first cells, which appear to have been present approximately three billion years ago. One particular time period in this range provides us a particularly interesting corollary for viral influences: the Late Archean.

A number of studies have detailed the removal of viruses from solution using iron oxides, mostly for the purposes of water treatment (e.g., Chang *et al.*, 1958; Manwaring *et al.*, 1971; You *et al.*, 2005; Zhu *et al.*, 2005). Viruses appear to adsorb to iron oxide particles through electrostatic attractions (Murray *et al.*, 1978; Ryan *et al.*, 2002; Shen *et al.*, 2010). The reactive sites are thought to be the carboxyl and amino functional groups on the viral capsid (Daughney *et al.*, 2004), but TEM images have also implicated phage tails, which may affect infectivity (Kyle *et al.*, 2008). This interaction is complicated by the high

surface area to volume ratio of iron and its numerous ligands – including phosphate and silica - which may compete with viruses for sorption sites (Daughney *et al.*, 2004; Konhauser *et al.*, 2007). The proclivity of viruses for hydrous iron oxide particles is particularly relevant to high-iron environments. Some have suggested the validity of the iron-virus interaction for environmental contexts (Gerba, 1984; Daughney *et al.*, 2004; Kyle *et al.*, 2008), but to our knowledge, ours is the first application to earth history.

In Late Archean and early Paleoproterozoic ocean basins, the deposition of banded iron formations is thought to result from a microbial iron cycle and a strong affinity of silica for ferric hydroxide sorption sites (Fischer & Knoll, 2009), leading to iron-silica co-precipitation and deposition in deep water sediments. Iron in surface waters is oxidized, attracts dissolved silica, and precipitates to depth, where iron respiration regenerates  $\text{Fe}^{2+}$  and releases silica before being recycled to the surface (Fischer & Knoll, 2009). This iron shuttle for silica has significant implications when we consider the proclivity of viruses to also sorb iron. Relatively anoxic conditions during this time allowed for high concentrations of dissolved iron (Holland, 1973). The exact amount of iron in Archean seawater is unknown but estimated at 0.05 mM (Holland, 1984) - a concentration comparable to the amounts used in laboratory techniques to flocculate viruses from seawater (John *et al.*, 2011).

Thus a suite of abiotic processes involving viral interaction with iron oxides and silica might be important for phage abundances and dynamics in iron-rich seawater. Recent studies have also pointed to important ramifications for a virus-mineral association, including loss of infectivity, shielding from UV inactivation, and impact on virus-host

correlations (Templeton *et al.*, 2006; Kyle *et al.*, 2008). Although the effect of high iron concentrations on dissolved phosphate in the Archean ocean has been investigated (Konhauser *et al.*, 2007), the effect on viruses has not.

Here we propose an experimental approach to quantify potential viral abundances in synthetic seawater solutions of varying iron and silica concentrations. Addition of silica complicates the simple iron-virus interaction described above by competing with viruses for sorption sites on the surface of hydrous iron oxide precipitates. This setup will also allow us to observe the behavior of silica and viruses in the absence of iron.

## 2. Methods

A known concentration of Syn33a cyanophages was introduced into each medium and the viral particles remaining in solution after a short centrifugation were enumerated using epifluorescence microscopy. This virus was chosen for its high relevance to ocean dynamics and previously sequenced genome (Sullivan *et al.*, 2010). Metal-free Aquil was used as our synthetic seawater within pH 7-8 (Morel *et al.*, 1979). The number of particles sequestered on the siliceous ferric oxide precipitate was estimated by difference, avoiding the need for resuspension. Our reductionist approach minimized potential complications, such as loss of virus while allowing for better efficiency.

### 2.1 Experimental design and centrifugation conditions

We simulated a total of 16 possible ocean conditions of varying iron and silica concentrations, spanning the range of likely Archean ocean amounts. This included  $[\text{Si}] = 0, 5, 80, 670 \mu\text{M}$  and  $[\text{Fe}] = 0, 20, 200, 2000 \mu\text{M}$ . Sixteen 50 ml polypropylene tubes containing 40 ml of approximately  $10^6$  viruses  $\text{ml}^{-1}$  and the corresponding iron and silica concentrations were prepared. After gentle shaking to allow the iron to precipitate, each tube was then centrifuged at 500g for 15 minutes. The supernatants were sampled, filtered, stained, and enumerated with SYBR Green (Figure 1). The precipitate was also sampled and stored in 1.5 ml tubes at  $-80^\circ\text{C}$ . This experiment was run in triplicate.

Despite the artificial complications, centrifugation was chosen over natural settling as the method for iron precipitation due to the inefficiency of settling reported in John *et al.* (2011). However, this required a control experiment to verify that our centrifugation conditions would only pellet those viruses adsorbed to iron particles. A test bottle of Fe

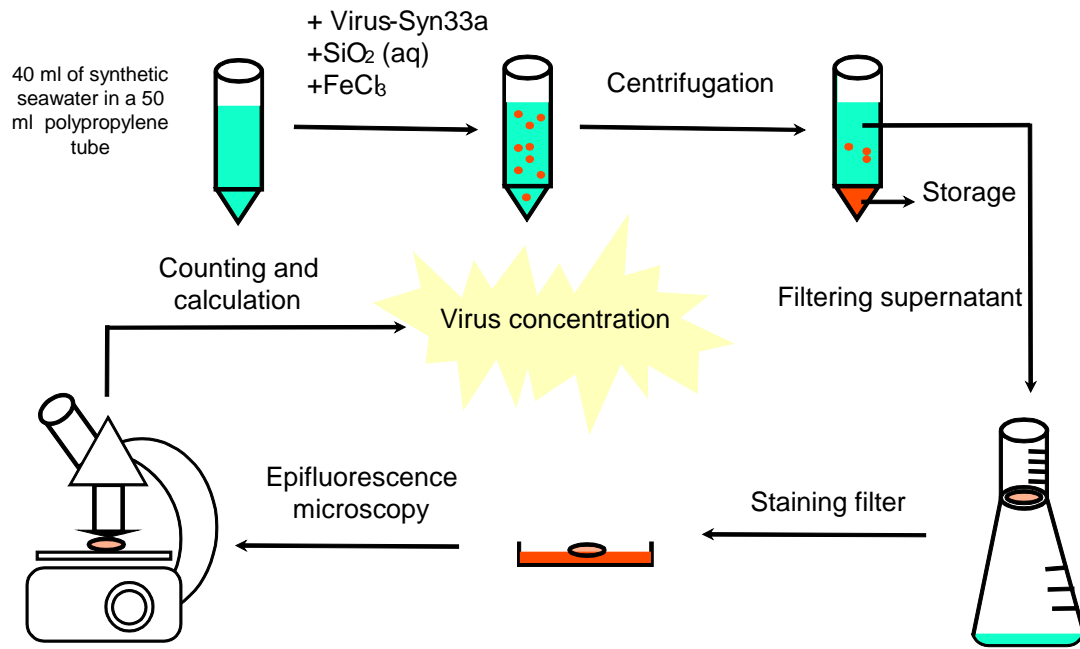


**Figure 1** Flowchart of developed simulation protocol. Following addition of virus, silica, and iron to Aquil<sup>6</sup>, each trial is shaken gently for iron to precipitate, then centrifuged and sampled for enumeration by epifluorescence microscopy.

2000  $\mu\text{M}$  seawater was centrifuged at varying conditions from speeds of 200-2000g and times 2-15 minutes. After each trial, the pellet was resuspended by gentle vortex and shaking. The pellet and supernatant were inspected for opacity and amount of iron pelleted to determine the ideal centrifugation condition that will pellet iron but not free-floating viruses. A potential candidate was 500g for 15 minutes, for which the supernatant was only very slightly opaque and similar to conditions involving 700g. There was no noticeable difference in opacity after 700g for 15 minutes. Using this information, the virus solution previously used for the wall-sticking control was centrifuged at 500g for 15 minutes. Samples were taken before and after centrifugation and counted. After testing these multiple centrifugation conditions, we established centrifugation at 500g for 15 minutes as our standard protocol. The discrepancy between virus concentration before ( $3.99 \times 10^7$  viruses  $\text{ml}^{-1}$ ) and after centrifugation ( $4.03 \times 10^7$  viruses  $\text{ml}^{-1}$ ) was attributed to error from lower virus number per FOV.

## **2.2 Wall effect determination**

Wall-sticking effects from the vessel used for the experiment were investigated. A 50 ml polypropylene tube holding 40 ml of virus solution (approximately  $10^7$  viruses  $\text{ml}^{-1}$ ) was prepared. Using epifluorescence microscopy, we tracked the number of viruses remaining in 40 ml of solution over 2 hours, sampling at times 0 (time of mixing/ inversion), 15 minutes, 30 minutes, 45 minutes, 1 hour, 1.5 hours, and 2 hours (Figure 2). Each time sample was diluted and fixed 1:50 in a 2 ml tube containing 0.02  $\mu\text{m}$ -filtered seawater and 2% formalin. We found up to a 29% decrease in virus concentration within one hour, ostensibly due to wall chemistry. Because the virus concentration remained within the same

order of magnitude ( $10^7$  viruses  $\text{ml}^{-1}$ ), we concluded that wall-sticking would not significantly alter our results under the set conditions.

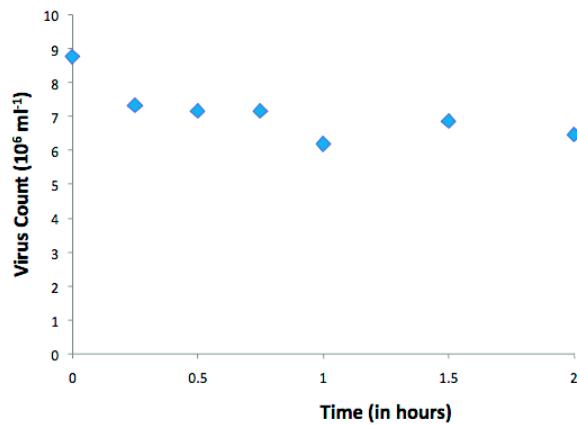


**Figure 2** Viruses remaining in solution over 2 hours using 40 mL of synthetic seawater in a 50 mL polypropylene tube. Virus concentration reliably decreased over time from  $8.8 \times 10^7$  to  $6.4 \times 10^7$  viruses  $\text{ml}^{-1}$ , with the exception of the 1 hour time point, which dipped unexpectedly to  $6.2 \times 10^7$ . This was attributed to observational error.

### 2.3 Silica and iron dissolution

Hydrochloric acid was used to facilitate dissolution of silica ( $\text{Na}_2\text{SiO}_3 \cdot 9\text{H}_2\text{O}$ ) in nanopure water. The maximum amount of hydrochloric acid in 40 ml of seawater media was calculated, assuming approximately  $2 \text{ mmol L}^{-1}$  of buffer. Stock solutions of silica were prepared in order for a 2 ml aliquot to yield 40 ml solutions of 0, 80, and  $670 \mu\text{M}$  silica. The synthetic seawater used in the experiments was metal- and silica-free Aquil medium (pH 7.95), prepared by S. John.

A concentrated iron stock of  $10 \text{ g L}^{-1} \text{ Fe}$  was prepared by dissolving  $\text{FeCl}_3 \cdot 6\text{H}_2\text{O}$  into nanopure water according to the recipe described in John *et al.* (2011). Varying amounts of this stock solution was then added to each trial to obtain the desired concentration.

### 2.4 Phage preparation

Phage strain Syn33a (a T4-like myovirus) grown on *Synechococcus* WH7803 arrived in four 15 ml tubes, which were immediately covered in foil and placed in  $8^\circ\text{C}$ . The tubes were numbered one through four and assumed to be separate batches. Batch 1 was noted to be significantly contaminated with bacteria, leading to crowding effects for high concentrations. Overall enumeration indicated a concentration of  $1.3 \times 10^8$  viruses  $\text{ml}^{-1}$ , and a 1:500 dilution was considered to be ideal for counts. We note that more than the usual 10 FOVs must be counted for accuracy. The three other virus batches were then enumerated using 1:500 dilutions. They were found to be relatively pure and not visibly contaminated with bacteria. Batch 2 was determined to have approximately  $8.8 \times 10^7$  viruses  $\text{ml}^{-1}$ , Batch 3

with  $1.1 \times 10^8$ , and Batch 4 with  $1.0 \times 10^8$ . These were deemed acceptable concentrations for approximating Archean seawater.

## **2.5 Enumeration by epifluorescence microscopy**

Virus flocculation was gauged by sampling the number of viruses left in the supernatant after precipitation and centrifugation. Following an established protocol (Patel *et al.*, 2007), dilutions were filtered and stained with SYBR Green I dsDNA/RNA dye, then enumerated using epifluorescence microscopy (Figure 1). All dilutions were made in a 2 ml centrifuge tube, inverted for mixing, and then very briefly spun down (4-6 seconds) in an Eppendorf centrifuge to minimize cap effects. For consistency, the same experimenter carried out each virus count.

### 3. Results

In the absence of silica, iron significantly reduced the number of viruses remaining in solution (Figures 3 and 4). This occurred across all three replicates, with percent differences dropping at least 31% when iron concentration increased from 20 to 200  $\mu\text{M}$ . Iron concentrations appeared to correlate with the amount of virus precipitated (Figure 3). For low iron conditions (0-20  $\mu\text{M}$ ), increasing silica concentrations past 5  $\mu\text{M}$  somewhat inhibited virus flocculation, although exact counts differed between replicates. Conditions of high silica and low iron consistently retained the most viruses in solution within each replicate (Figure A1). However, for intermediate iron concentrations around 200  $\mu\text{M}$  (Figures 3 and 5), high amounts of silica (670  $\mu\text{M}$ ) significantly rescued virus numbers to values seen in low iron conditions. This effect disappeared when the iron concentration was raised to 2000  $\mu\text{M}$  of iron: high iron conditions (2000  $\mu\text{M}$ ) consistently precipitated the vast majority of viruses (percent differences of -97 to -100), even for the highest amounts of silica (Figures 3 and 4). These four trials also had the lowest standard deviations, ranging from 0 to 1.15 (Figure A2). We note that samples with low virus concentrations, especially those containing 2000  $\mu\text{M}$  Fe, may have a higher degree of error because counts could not reach the recommended 200 viruses per slide for accuracy.

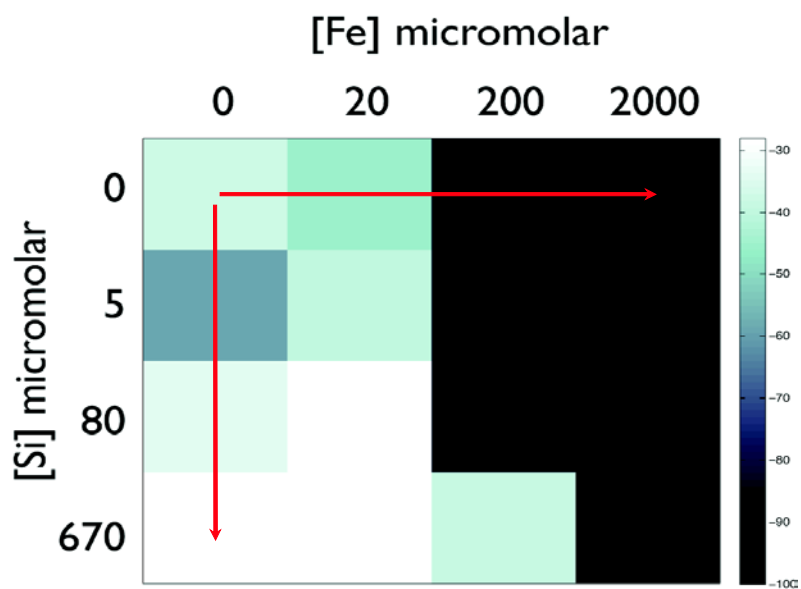


**Figure 3** Colormap of averaged percent differences. For each trial, percent differences from starting concentrations were calculated and averaged across the triplicate. Standard deviations are listed in Figure A2.

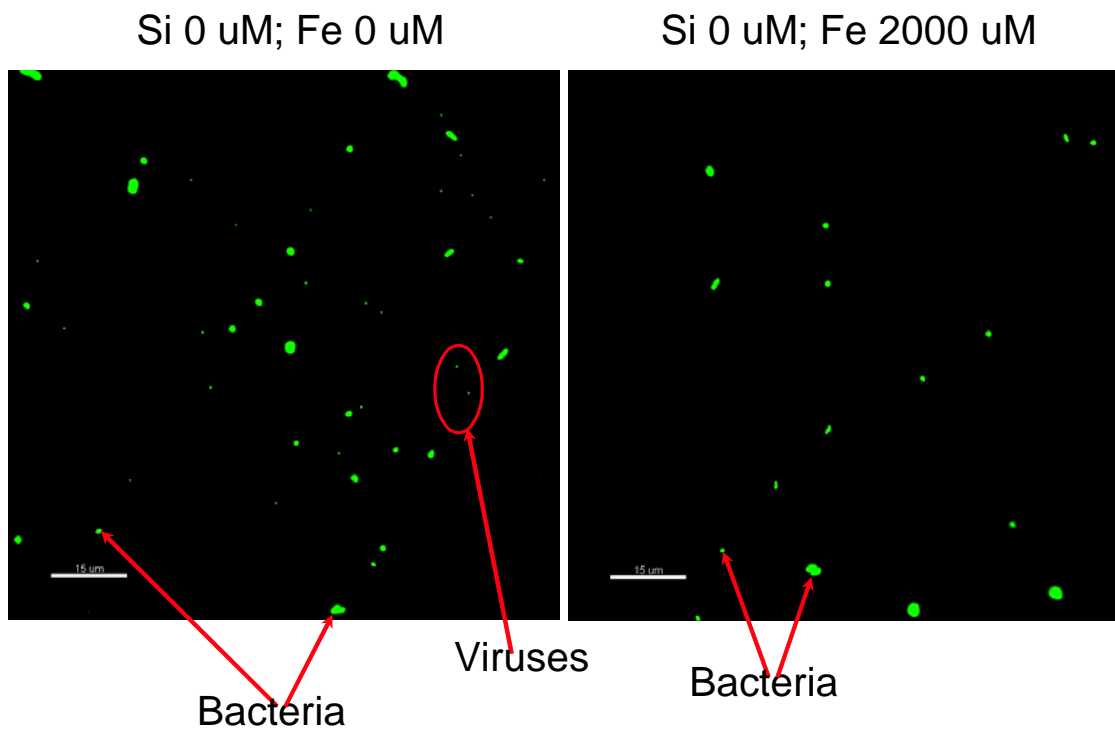


**Figure 4** Comparison of epifluorescence images with and without iron addition.

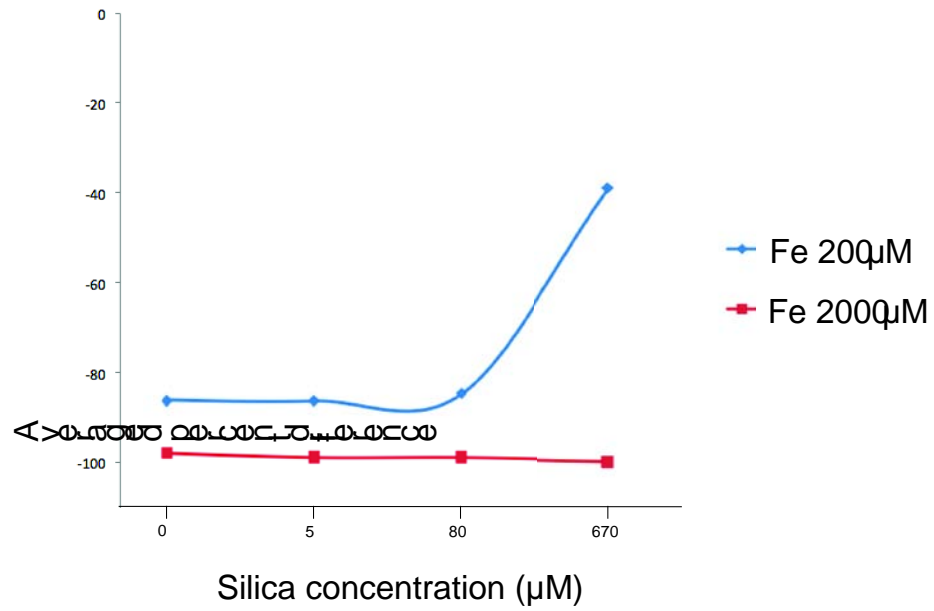


**Figure 5** Trends in Fe 200 and 2000 uM. Comparison of averaged percent differences between two highest concentrations of iron with increasing silica. Silica concentrations not to scale.

## 4. Discussion

### 4.1 Abiotic processes occurring in the Archean ocean

The limited inhibition of virus flocculation by silica suggests the existence of an iron threshold or saturation point between 200 and 2000  $\mu\text{M}$ , beyond which any addition of silica can no longer affect virus flocculation. This supports the idea that viruses and silica are competing for a limited number of iron sorption sites, a phenomenon that may well have happened in the Archean ocean. As stromatolites, what we know as accretionary structures of cyanobacteria, are the earliest known evidence of life and have been traced to around 3 Ga (Noffke *et al.*, 2003; Schopf, 2006), the use of cyanophage for this experiment appears to be highly pertinent. However, the earliest stromatolites may have been anoxygenic and true cyanophages only present at 2.4 Ga (Schopf, 2011). In addition, the morphology of Syn33a, a T4-like bacteriophage, is relatively complex, and we hope to replicate these results with siphovirus and podovirus, among other viruses that may better represent evolutionarily ancient viruses. Since the majority of viruses we know of are polyvalent, heterophages may be a more realistic option. Different species of viruses vary in their surface chemistry and resulting interactions with iron (Gerba, 1984; Kyle *et al.*, 2008), and it would be interesting to investigate how virus morphology correlates with iron interaction. We plan to refine our silica and iron parameters to narrow in on the Fe 200-2000  $\mu\text{M}$  range. This will allow us to study virus dynamics close to the threshold of silica competition. Experiments using starting virus concentrations closer to the modern average for seawater ( $10^7$ - $10^8$  viruses  $\text{ml}^{-1}$ ) may also help more realistically characterize the

interactions between virus, silica, and iron. Future work will include modeling the effects of the iron-virus-silica interaction on biogeochemical cycles such as the biological pump.

#### **4.2 Elemental ratios of cyanophage**

We undertook a theoretical calculation of the carbon, nitrogen, and phosphorus content of our phage, loosely based on the calculation for Turnip Yellow Mosaic Virus (Symons *et al.*, 1963; Kaper & Litjens, 1966). Our approach is based on the assumption that the phage is composed of three parts: capsid, DNA, and proteins/polyamines. Excluding polyamines and non-capsid proteins, the approximate C:N:P ratio was determined to be approximately 25.2 : 7.8 : 1. Syn33 data were used for the DNA calculation, but T4 phage data were used for the capsid proteins (Leiman *et al.*, 2003; Sullivan *et al.*, 2010). Our calculation demonstrated that the virus is enriched in phosphorus relative to the Redfield ratio of 106:16 :1, which is generally considered as a measure of ocean biology (Redfield, 1934; Redfield, 1958; Arrigo, 2005). The virus-iron interaction may therefore have had a significant influence on the biogeochemistry of the Archean ocean. This abiotic process may have been responsible for depositing phosphorus to sediment in the form of viruses and contributing to the phosphorus signals we see in BIFs today (Planavsky *et al.*, 2010).

#### **4.3 Modern significance**

The interaction between virus, silica, and iron has the potential to substantially alter virus-host interactions in modern environments as well. Extensive virus mineralization by iron has been reported in the Rio Tinto, resulting in possible loss of infectivity (Kyle *et al.*, 2008). Hot springs depositing silica are predicted to silicify the capsids of T4

bacteriophages, which can compromise infectivity and lead to lowered microbial diversity (Laidler & Stedman, 2010). Laidler and Stedman (2010) also suggest that viruses located in such environments might adapt to evade silicification and subsequent inactivation. It remains to be seen whether silicification or mineralization can help preserve viruses in the rock record.

We note that addition of silica to low concentrations of iron (0-20  $\mu\text{M}$ ) appears to have a slight inhibitory effect, constituting the least percent differences of all trials. The mechanism for inhibition is unknown but may involve a decrease in wall-sticking effects or the formation of virus-silica complexes. Addition of silica may prove to be a potentially useful technique for improving virus recovery under laboratory conditions. On a microscopic level, TEM on collected precipitates from the current experiment (Figure 1) may help visualize this association.

Finally, the effect of iron on a mixed population of bacteria and virus should be investigated. Although studies have demonstrated the adsorption of iron to bacterial surfaces (e.g., Wightman & Fein, 2005), bacterial concentrations observed from the supernatant post-centrifugation were not noticeably affected by the addition of iron (Figure 4). It is yet unclear whether iron selectively flocculates viruses from a heterogenous solution.

## Conclusions

We set out to examine the influence of abiotic interactions between virus and iron on the abundance and behavior of Archean viruses. To inform this problem, a set of simple competition experiments were implemented for iron and silica concentrations of interest. We confirm that greater amounts of iron lead to increased virus flocculation, and while sufficiently high concentrations of silica (670  $\mu\text{M}$ ) managed to inhibit precipitation of virus up to 200  $\mu\text{M}$  Fe, this effect was undetectable for 2000  $\mu\text{M}$  Fe. Our results suggest a concentration-dependent competition between virus and silica for iron sorption sites and present a novel concept of viral involvement in Archean iron cycles as well as modern iron-rich environments. It remains to be seen how this interaction plays out for different phage morphologies as well as modern-day virus concentrations.

## BIBLIOGRAPHY

- Arrigo KR (2005) Marine microorganisms and global nutrient cycles. *Nature*, **437**, 349-355.
- Benson SD, Bamford JKH, Bamford DH, Burnett RM (2004) Does common architecture reveal a viral lineage spanning all three domains of life? *Mol Cell*, **16**, 673-685.
- Bidle KD, Haramaty L, Ramos JBE, Falkowski P (2007) Viral activation and recruitment of metacaspases in the unicellular coccolithophore, *Emiliana huxleyi*. *P Natl Acad Sci USA*, **104**, 6049-6054.
- Breitbart M, Miyake JH, Rohwer F (2004) Global distribution of nearly identical phage-encoded DNA sequences. *Fems Microbiol Lett*, **236**, 249-256.
- Brocks JJ, Buick R, Summons RE, Logan GA (2003) A reconstruction of Archean biological diversity based on molecular fossils from the 2.78 to 2.45 billion-year-old Mount Bruce Supergroup, Hamersley Basin, Western Australia. *Geochim Cosmochim Acta*, **67**, 4321-4335.
- Brocks JJ, Logan GA, Buick R, Summons RE (1999) Archean molecular fossils and the early rise of eukaryotes. *Science*, **285**, 1033-1036.
- Brussaard CPD, Wilhelm SW, Thingstad F, Weinbauer MG, Bratbak G, Heldal M, Kimmance SA, Middelboe M, Nagasaki K, Paul JH, Schroeder DC, Suttle CA, Vaque D, Wommack KE (2008) Global-scale processes with a nanoscale drive: The role of marine viruses. *Isme J*, **2**, 575-578.
- Chang SL, Stevenson RE, Bryant AR, Woodward RL, Kabler PW (1958) Removal of Cocksackie and bacterial viruses and the native bacteria in raw Ohio River water by flocculation with aluminum sulfate and ferric-chloride. *Am J Public Health N*, **48**, 159-169.
- Chiura HX (1997) Generalized gene transfer by virus-like particles from marine bacteria. *Aquat Microb Ecol*, **13**, 75-83.
- Chiura HX (2002) Broad host range xenotrophic gene transfer by virus-like particles from a hot spring. *Microbes Environ*, **17**, 53-58.
- Coleman ML, Sullivan MB, Martiny AC, Steglich C, Barry K, Delong EF, Chisholm SW (2006) Genomic islands and the ecology and evolution of *Prochlorococcus*. *Science*, **311**, 1768-1770.
- Daughney CJ, Chatellier X, Chan A, Kenward P, Fortin D, Suttle CA, Fowle DA (2004) Adsorption and precipitation of iron from seawater on a marine bacteriophage (PWH3A-P1). *Mar Chem*, **91**, 101-115.
- Filee J, Forterre P, Sen-Lin T, Laurent J (2002) Evolution of DNA polymerase families: Evidences for multiple gene exchange between cellular and viral proteins. *J Mol Evol*, **54**, 763-773.
- Fischer WW, Knoll AH (2009) An iron shuttle for deepwater silica in Late Archean and early Paleoproterozoic iron formation. *Geol Soc Am Bull*, **121**, 222-235.

- Frada M, Probert I, Allen MJ, Wilson WH, De Vargas C (2008) The "Cheshire Cat" escape strategy of the coccolithophore *Emiliania huxleyi* in response to viral infection. *P Natl Acad Sci USA*, **105**, 15944-15949.
- Fuhrman JA (1999) Marine viruses and their biogeochemical and ecological effects. *Nature*, **399**, 541-548.
- Gerba CP (1984) Applied and theoretical aspects of virus adsorption to surfaces. *Adv Appl Microbiol*, **30**, 133-168.
- Gobler CJ, Hutchins DA, Fisher NS, Coper EM, Sanudo-Wilhelmy SA (1997) Release and bioavailability of C, N, P, Se, and Fe following viral lysis of a marine chrysophyte. *Limnol Oceanogr*, **42**, 1492-1504.
- Hendrix RW, Smith MCM, Burns RN, Ford ME, Hatfull GF (1999) Evolutionary relationships among diverse bacteriophages and prophages: All the world's a phage. *P Natl Acad Sci USA*, **96**, 2192-2197.
- Hill RW, White BA, Cottrell MT, Dacey JWH (1998) Virus-mediated total release of dimethylsulfoniopropionate from marine phytoplankton: A potential climate process. *Aquat Microb Ecol*, **14**, 1-6.
- Holland HD (1973) The Oceans: A possible source of iron in iron-formations. *Econ Geol*, **68**, 1169-1172.
- Holland HD (1984) *The Chemical Evolution of the Atmosphere and Oceans*, Princeton University Press.
- Holmes EC (2003) Molecular clocks and the puzzle of RNA virus origins. *J Virol*, **77**, 3893-3897.
- Jiang SC, Paul JH (1998) Gene transfer by transduction in the marine environment. *Appl Environ Microb*, **64**, 2780-2787.
- John SG, Mendez CB, Deng L, Poulos B, Kauffman AKM, Kern S, Brum J, Polz MF, Boyle EA, Sullivan MB (2011) A simple and efficient method for concentration of ocean viruses by chemical flocculation. *Env Microbiol Rep*, **3**, 195-202.
- Kaper JM, Litjens EC (1966) Ribonucleic acid content of Turnip Yellow Mosaic Virus. *Biochemistry-U.S*, **5**, 1612-1617.
- Konhauser KO, Lalonde SV, Amskold L, Holland HD (2007) Was there really an Archean phosphate crisis? *Science*, **315**, 1234-1234.
- Kyle JE, Pedersen K, Ferris FG (2008) Virus mineralization at low pH in the Rio Tinto, Spain. *Geomicrobiol J*, **25**, 338-345.
- Laidler JR, Stedman KM (2010) Virus silicification under simulated hot spring conditions. *Astrobiology*, **10**, 569-576.
- Leiman PG, Kanamaru S, Mesyanzhinov VV, Arisaka F, Rossmann MG (2003) Structure and morphogenesis of bacteriophage T4. *Cell Mol Life Sci*, **60**, 2356-2370.
- Manwaring JF, Chaudhuri M, Engelbrecht R (1971) Removal of viruses by coagulation and flocculation. *J Am Water Works Ass*, **63**, 298-300.
- Morel FMM, Rueter JG, Anderson DM, Guillard RRL (1979) Aquil - chemically defined phytoplankton culture-medium for trace-metal studies. *J Phycol*, **15**,

135-141.

- Murray JP, Parks GA, Schwerdt CE (1978) Poliovirus adsorption on oxide surfaces. *Abstr Pap Am Chem S*, **175**, 24-24.
- Noffke N, Hazen R, Nhleko N (2003) Earth's earliest microbial mats in a siliciclastic marine environment (2.9 Ga Mozaan Group, South Africa). *Geology*, **31**, 673-676.
- Patel A, Noble RT, Steele JA, Schwalbach MS, Hewson I, Fuhrman JA (2007) Virus and prokaryote enumeration from planktonic aquatic environments by epifluorescence microscopy with SYBR Green I. *Nat Protoc*, **2**, 269-276.
- Peduzzi P, Weinbauer MG (1993) The submicron size fraction of seawater containing high numbers of virus-particles as bioactive agent in unicellular plankton community successions. *J Plankton Res*, **15**, 1375-1386.
- Planavsky NJ, Rouxel OJ, Bekker A, Lalonde SV, Konhauser KO, Reinhard CT, Lyons TW (2010) The evolution of the marine phosphate reservoir. *Nature*, **467**, 1088-1090.
- Poinar G, Poinar R (2005) Fossil evidence of insect pathogens. *J Invertebr Pathol*, **89**, 243-250.
- Poorvin L, Rinta-Kanto JM, Hutchins DA, Wilhelm SW (2004) Viral release of iron and its bioavailability to marine plankton. *Limnol Oceanogr*, **49**, 1734-1741.
- Redfield AC (1934) On the proportions of organic derivations in sea water and their relation to the composition of plankton. In: *James Johnstone Memorial Volume* (ed Daniel RJ). Liverpool University Press, pp. 176-192.
- Redfield AC (1958) The biological control of chemical factors in the environment. *Am Sci*, **46**, 205-221.
- Rice G, Tang L, Stedman K, Roberto F, Spuhler J, Gillitzer E, Johnson JE, Douglas T, Young M (2004) The structure of a thermophilic archaeal virus shows a double-stranded DNA viral capsid type that spans all domains of life. *P Natl Acad Sci USA*, **101**, 7716-7720.
- Rohwer F, Thurber RV (2009) Viruses manipulate the marine environment. *Nature*, **459**, 207-212.
- Ryan JN, Harvey RW, Metge D, Elimelech M, Navigato T, Pieper AP (2002) Field and laboratory investigations of inactivation of viruses (PRD1 and MS2) attached to iron oxide-coated quartz sand. *Environ Sci Technol*, **36**, 2403-2413.
- Schopf JW (2006) Fossil evidence of Archaean life. *Philos T R Soc B*, **361**, 869-885.
- Schopf JW (2011) The paleobiological record of photosynthesis. *Photosynth Res*, **107**, 87-101.
- Shen LL, Zhao BZ, Zhang JB, Chen J, Zheng H (2010) Virus adsorption onto nano-sized iron oxides as affected by different background solutions. *Huan Jing Ke Xue*, **31**, 983-989.
- Short CM, Suttle CA (2005) Nearly identical bacteriophage structural gene

- sequences are widely distributed in both marine and freshwater environments. *Appl Environ Microb*, **71**, 480-486.
- Sullivan MB, Coleman ML, Weigele P, Rohwer F, Chisholm SW (2005) Three *Prochlorococcus* cyanophage genomes: Signature features and ecological interpretations. *Plos Biol*, **3**, 790-806.
- Sullivan MB, Huang KH, Ignacio-Espinoza JC, Berlin AM, Kelly L, Weigele PR, Defrancesco AS, Kern SE, Thompson LR, Young S, Yandava C, Fu R, Krastins B, Chase M, Sarracino D, Osburne MS, Henn MR, Chisholm SW (2010) Genomic analysis of oceanic cyanobacterial myoviruses compared with T4-like myoviruses from diverse hosts and environments. *Environ Microbiol*, **12**, 3035-3056.
- Suttle CA (2005) Viruses in the sea. *Nature*, **437**, 356-361.
- Suttle CA (2007) Marine viruses - major players in the global ecosystem. *Nat Rev Microbiol*, **5**, 801-812.
- Symons RH, Short MN, Markham R, Rees MW (1963) Relationships between ribonucleic acid and protein of some plant viruses. *J Mol Biol*, **6**, 1-15.
- Templeton MR, Andrews RC, Hofmann R (2006) Impact of iron particles in groundwater on the UV inactivation of bacteriophages MS2 and T4. *J Appl Microbiol*, **101**, 732-741.
- Thingstad TF (2000) Elements of a theory for the mechanisms controlling abundance, diversity, and biogeochemical role of lytic bacterial viruses in aquatic systems. *Limnol Oceanogr*, **45**, 1320-1328.
- Van Hannen EJ, Zwart G, Van Agterveld MP, Gons HJ, Ebert J, Laanbroek HJ (1999) Changes in bacterial and eukaryotic community structure after mass lysis of filamentous cyanobacteria associated with viruses. *Appl Environ Microb*, **65**, 795-801.
- Waldor MK, Friedman DI, Adhya SL (2005) Phages: Their role in bacterial pathogenesis and biotechnology. ASM Press.
- Weinbauer MG (2004) Ecology of prokaryotic viruses. *Fems Microbiol Rev*, **28**, 127-181.
- Wightman PG, Fein JB (2005) Iron adsorption by *Bacillus subtilis* bacterial cell walls. *Chem Geol*, **216**, 177-189.
- Wilcox RM, Fuhrman JA (1994) Bacterial-viruses in coastal seawater - lytic rather than lysogenic production. *Mar Ecol-Prog Ser*, **114**, 35-45.
- Wilhelm SW, Suttle CA (1999) Viruses and nutrient cycles in the sea - viruses play critical roles in the structure and function of aquatic food webs. *Bioscience*, **49**, 781-788.
- You Y, Han J, Chiu PC, Jin Y (2005) Removal and inactivation of waterborne viruses using zerovalent iron. *Environ Sci Technol*, **39**, 9263-9269.
- Zhu BT, Clifford DA, Chellam S (2005) Virus removal by iron coagulation-microfiltration. *Water Res*, **39**, 5153-5161.

## Appendix: Additional Figures

**Figure A1** Percent differences from starting concentrations for individual experiment replicates. Since we are estimating the amount of virus flocculated by difference, counts represented here have negative percent differences.

Experiment 1	Si\Fe	0	20	200	2000
	0	-34	-30	-88	-99
	5	-68	-25	-91	-100
	80	-31	-19	-99	-100
	670	-28	-23	-50	-100
Experiment 2	Si\Fe	0	20	200	2000
	0	-50	-59	-93	-97
	5	-60	-47	-81	-99
	80	-45	-38	-68	-99
	670	-31	-33	-41	-100
Experiment 3	Si\Fe	0	20	200	2000
	0	-30	-47	-78	-99
	5	-48	-48	-87	-99
	80	-25	-29	-87	-99
	670	-28	-28	-26	-100

**Figure A2** Standard deviations of percent differences across triplicate. The maximum deviation observed was 15.6, for the condition 80uM Si – 200 uM Fe. Deviations for 2000 uM Fe and the 670 uM Si - 0 uM Fe trials were particularly low. The overall standard deviation (averaged) was approximately 7.3%.

Si\Fe	0	20	200	2000
0	10.5830052	14.571662	7.63762616	1.15470054
5	10.0664459	13	5.03322296	0.57735027
80	10.2632029	9.50438495	15.6311655	0.57735027
670	1.73205081	5	12.1243557	0